K-9-5

Extended Abstracts of the 2011 International Conference on Solid State Devices and Materials, Nagoya, 2011, pp1302-1303

RF Performance of Graphene Nano-Ribbon MOSFET vs. TFET

Vijayashree Parsi Sreenivas, Kai Tak Lam* and Liang Gengchiau†

Computational Nanoelectronic and Nano-device Lab, Department of Electrical and Computer Engineering,
National University of Singapore, Singapore 119260, Republic of Singapore
Phone: +65 65162898, Fax: +65 65162104, Email: *lamkt@nus.edu.sg and †elelg@nus.edu.sg

1. Introduction

Scaling of silicon based electronic devices is approaching its limits and there is a rising need to extend the study of conventional CMOS to alternative channel materials. Graphene has been intensively studied and appreciated for its high carrier mobility and saturation velocity which makes it ideal for post silicon nanoelectronics. Recent studies [1-5] have suggested that the high mobility of graphene-based materials makes them suitable for high-frequency (RF) device applications and an operation frequency of graphene FET (GFET) in the gigahertz range has been reported [4]. However, due to a lack of saturation current [5], the gain of graphene MOSFET is limited by the drain conductance. For RF amplifier, semi-conducting graphene nanoribbon (GNR) might be a better candidate due to the presence of energy band gap (E_G) which provides a lower drain conductance at saturation, and hence a higher gain. In this paper, we discuss the gain and operation frequency of GNR devices at different ribbon widths. Apart from the conventional MOSFET device structure, GNR tunneling FET (TFET) is also simulated for comparison.

2. Simulation Approach

The device performance of GNR MOSFETs and TFETs are investigated using quantum transport simulator based on the non-equilibrium Green's function (NEGF) formalism [6] in the ballistic regime coupled with a mode-space Dirac tight-binding model [7]. The electrostatic potential is obtained self-consistently from a two dimensional Poisson solver [8]. The cross-section schematic of the device simulated is shown in Fig. 1. A double-gated planar structure is used, with SiO_2 ($\varepsilon_r = 4$) as the insulating material. GNR of widths (W) 1 to 4 nm are investigated and their E_G, effective masses (m^*) and device threshold voltage (V_t) are shown in the table of Fig. 1. The doping concentrations at the source and drain are symmetric at 6.87×10^{10} cm^{-2} for a shift in the Fermi level by 0.2 eV above (below) the conduction (valence) band of the n-type (p-type) doped contacts. The GNR MOSFETs have an n-i-n device structure while the TFETs are p-i-n. For the RF performance evaluation, the transconductance (g_m), operation frequency (f_T), drain conductance (g_d) and gain (A_V) are:

$$g_m = \frac{dI_{DS}}{dV_{GS}},\ f_T = \frac{g_m}{2\pi C_G},\ g_d = \frac{dI_{DS}}{dV_{DS}},\ A_V = \frac{g_m}{g_d}. \quad (1)\text{-}(4)$$

Drain current (I_{DS}) at bias steps of 10 mV are used for conductance calculations, with the drain bias (V_{DS}) fixed at 0.1 V for g_m and gate bias (V_{GS}-V_t) fixed at 0.1 V for g_d. The C_G is the gate capacitance which includes both the oxide and quantum capacitances.

3. Results and Discussion

(A) MOSFET simulations: The RF performances of GNR MOSFET are firstly shown in Fig. 2. It is observed that for all V_{GS} investigated, the g_m increases with the width of GNR [Fig. 2(a)]. This is due to the smaller E_G of wider GNR which provides a smaller effective mass, resulting in a higher carrier velocity and I_{DS}. As a result, the f_T of GNR MOSFET increases from 523 GHz to 3.07 THz as the ribbon width increases from 1 to 4 nm [Fig. 2(b)]. On the other hand, as V_{DS} increases, the g_d decreases for $W = 1$ nm but it increases for $W = 4$ nm [Fig. 2(c)]. To understand this phenomenon, the I_{DS}-V_{DS} plots are shown in Fig. 3(a) and the non-saturation of I_{DS} for 2.8 and 4 nm devices is observed which contributes to the increase in g_d. This is due to the band-to-band tunneling (BTBT) of small E_G material at high V_{DS} [cf. Fig. 3(d) and 3(e)]. Furthermore, in general, the g_d is higher for wider GNR, which leads to a decrease of maximum A_v from 14.8 to 5.45 as ribbon width increases. It indicates that careful designs and control bias is important to practically implement GFETs in RF applications.

(B) TFET simulations: The RF performances of GNR TFET are examined next in Fig. 4. Similar to GNR MOSFET, the g_m, f_T and g_d of GNR TFET increase with the ribbon width while A_V decreases with it. While the g_m of TFET is, in general, lower than that of MOSFET, their f_T are similar due to a smaller C_G of TFET. On the other hand, the g_d of GNR TFETs with narrow widths are lower than MOSFET due to a more saturated I_{DS} of TFET. This leads to a higher A_V for the narrow ribbon TFETs. However, for wider TFETs, due to the high BTBT current at the channel/drain (C/D) interface [Fig. 5(d) and 5(e)], g_d of the device increases, resulting in a lowering of the A_V to the similar level of MOSFET. However, we noted that the BTBT at the C/D interface could be reduced by lowering the drain doping concentration [9], and A_V could be increased.

4. Summary

The RF performances of GNR MOSFET and TFETs at different ribbon widths are summarized in Table 1. Although the devices exhibits increased frequency performances at wider ribbon widths, the gain is degraded due to a higher drain conductance. For narrow ribbon widths, the GNR TFETs give a better gain than MOSFETs operating at a similar frequency due to more saturated I_{DS}. Narrow width GNR FETs might be a better choice for RF amplifier applications due to the finite energy gap.

References

[1] F. Schwierz, Nature Nanotechnol., 5 487 (2010).
[2] I. Meric, *et al.*, 10.1109/IEDM.2008.4796738 (2008).
[3] Y.-M. Lin, *et al.*, 10.1109/IEDM.2009.5424378 (2009).
[4] Y.-M. Lin, *et al.*, Nano Lett. 9, 422 (2009).
[5] I. Imperiale, *et al.*, 10.1109/IEDM.2010.5703463 (2010).
[6] S.Datta, *Quantum Transport: Atom to Transistor* (2005).
[7] S. K. Chin, *et al.*, IEEE Trans. Electron Dev. 57, 3144 (2010).
[8] K. T. Lam, *et al.*, IEE Electron Dev. Lett. 32, 431 (2011).
[9] K. T. Lam, *et al.*, Jpn. J. Appl. Phys. 49, 04DJ10 (2009).

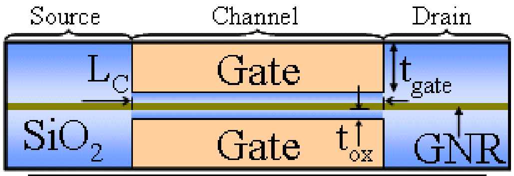

W (nm)	E_G (eV)	m^*/m_0	V_t (V)
1.0	0.874	3.69×10^{-2}	0.27
1.8	0.549	2.49×10^{-2}	0.15
2.6	0.400	1.87×10^{-2}	0.10
4.0	0.259	1.27×10^{-2}	0.03

Fig. 1 A cross-section schematic of the graphene nanoribbon (GNR) double-gate devices where t_{gate} = 3 nm, t_{ox} = 1 nm and L_C = 16 nm. Table of the different ribbon widths (W) used and their corresponding band gaps (E_G), normalized effective mass (m^*) and calculated threshold voltages (V_t) corresponding to each width.

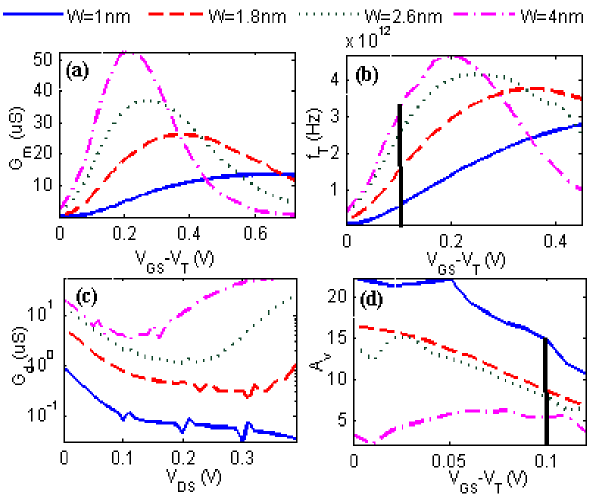

Fig. 2 : Plots of (a) transconductance (g_m) vs. V_{GS} (b) frequency (f_T) vs. V_{GS} (c) drain conductance (g_d) vs. V_{DS} (d) gain (A_V) vs. V_{GS} of the MOSFET for different widths of GNR.

Table 1 RF performance of GNR MOSFET and TFET.

	W (nm)	g_m (µS)	g_d (nS)	f_T (THz)	A_v
MOS-FET	**1.0**	1.18	0.0802	0.523	14.8
	1.8	6.59	0.761	1.47	8.68
	2.6	15.8	2.00	2.43	7.92
	4.0	25.5	4.00	3.07	5.45
T-FET	**1.0**	0.376	0.00934	0.218	40.4
	1.8	3.32	0.197	9.52	16.8
	2.6	9.18	0.847	1.84	10.9
	4.0	15.7	3.17	2.25	5.55

(Note: All values taken at V_{DS} = 0.1 V, V_{GS}-V_t= 0.1 V)

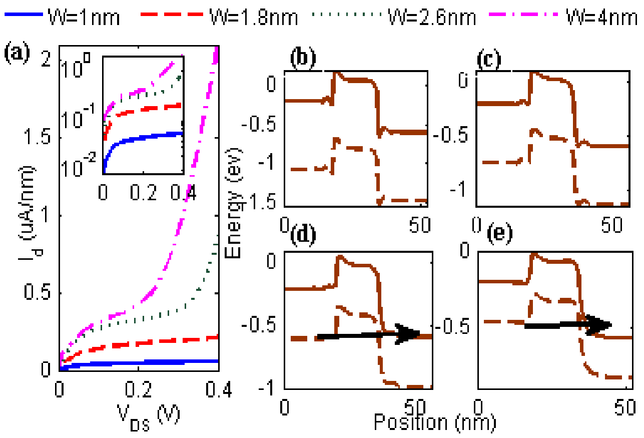

Fig. 3: (a) Comparison of the current characteristics for different widths of MOSFET at a constant V_{GS}-V_t = 0.1 V. Potential profiles showing the effect of BTBT at different ribbon widths (in nm): (b) 1.0 (c) 1.8 (d) 2.6 (e) 4.0 at V_{DS} = 0.4 V and V_{GS}-V_t = 0.1V.

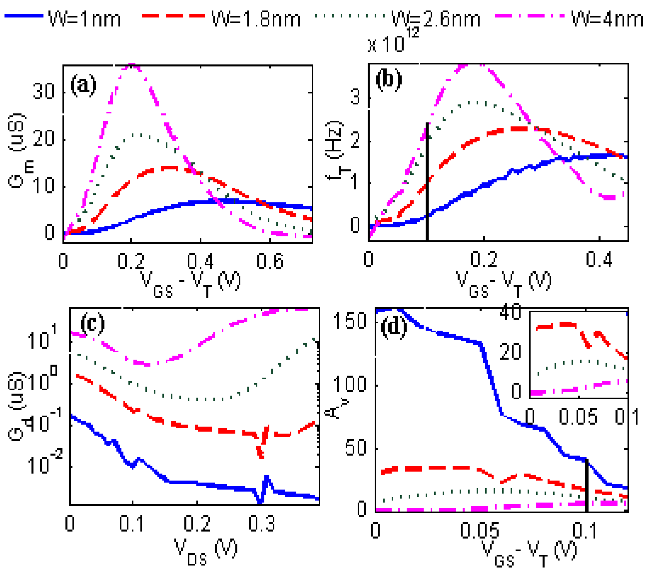

Fig. 4 Plots of (a) g_m vs. V_{GS} (b) f_T vs. V_{GS} (c) g_d vs. V_{DS} (d) A_V vs. V_{GS} of the TFET for different widths of GNR.

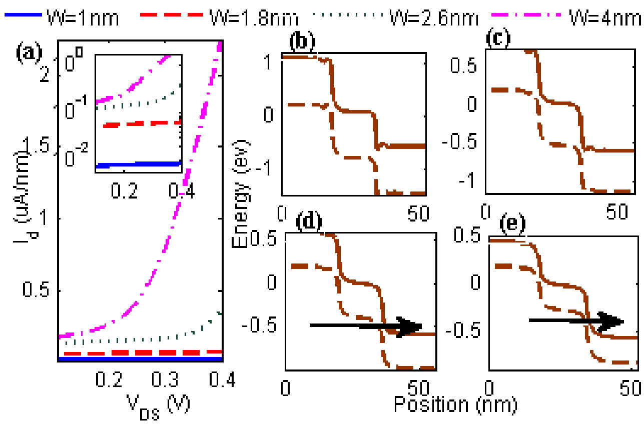

Fig. 5: (a) Comparison of the current characteristics for different widths of TFET at a constant V_{GS}-V_t = 0.1 V. Potential profiles showing the effect of BTBT at different ribbon widths (in nm): (b) 1.0 (c) 1.8 (d) 2.6 (e) 4.0 at V_{DS} = 0.4 V and V_{GS}-V_t = 0.1 V.